energies

MDPI

Review

Biological and Medical Disturbances Due to Exposure to Fields Emitted by Electromagnetic Energy Devices—A Review

Adel Razek

Group of Electrical Engineering–Paris (GeePs), CNRS, University of Paris-Saclay and Sorbonne University, F91190 Gif sur Yvette, France; adel.razek@centralesupelec.fr

Abstract: The use of electromagnetic systems in daily life is on the rise. The immediate environment, of these electromagnetic energy devices, is exposed to their emitted fields. Environmental disturbances from such exposure could be severe in many ways; one of the most important is health. This could be directly related to the human body or to healthcare sensing and interventional devices. The review of the biological effects and disturbances of medical instruments due to electromagnetic field exposure is the subject of this article. The analysis of the different types of exposure as well as their control to meet safety requirements are investigated involving energy devices covering wide ranges of power and frequency. Thus, biological effects of both wireless telecommunications tools and inductive charging systems are reviewed. Next, we survey electromagnetic disturbances in sensing and stimulation instruments joint to the human body as well as devices used in medical interventions. Means of evaluating and controlling the effects of electromagnetic fields, through electromagnetic compatibility analysis, experimentally and by numerical modeling are conferred and assessed.

Keywords: energy devices; radiated fields; electromagnetic field exposure; biological effects; medical instruments disturbance; EMC

Citation: Razek, A. Biological and Medical Disturbances Due to Exposure to Fields Emitted by Electromagnetic Energy Devices—A Review. *Energies* **2022**, *15*, 4455. https://doi.org/10.3390/en15124455

Academic Editor: Anastasios Dounis

Received: 6 May 2022
Accepted: 17 June 2022
Published: 18 June 2022

1. Introduction

With the increase in the practice of electromagnetic fields (EMFs) in daily life, many research efforts regarding their effects have been devoted in different fields. One of the most important is the area of health. The investigations focused on the interactions between electromagnetic (EM) sources and, the human body on the one hand and health instruments on the other. Three issues generally motivate assessments of EMFs exposure effects. The first is to evaluate the fields induced in the human body at the frequency and power of the source in order to assess the potential effects on health in accordance with the international standards [1–3]. The second issue is to evaluate the risk of disturbance of medical devices, integrated (or combined) with the body, used in therapeutics or involved in interventions. The last issue concerns the evaluation of the influence of the source on the radiation levels permitting to stipulate the data to determine the degree of freedom in the design and the optimization of the source systems. The effects of EMFs exposure are strongly related to both natures of the EMF and the matter exposed. The EMF nature, for a given radiated power, concerns the field strength and its wave frequency and form. The matter-exposed nature is related to its physical properties and geometric aspect.

Regarding the human body exposure to the EMF environment, generally the most concerned devices are those exercising important stray fields like wireless energy transfer apparatuses. These involve wide ranges of power and frequency. Two key cases are concerned that, telecommunication and wireless inductive energy transfer. The case of telecommunications involve common sources such as RF radiation emitted by antennas, Wi-Fi access points, smartphones, tablets, portable phones and Bluetooth devices. As the used frequencies in these apparatuses are relatively high and the exposed object concerns the human head and body, we have to control the security conditions of these devices,

see e.g., [4–9]. The second case relates to wireless inductive charging systems for applications ranging from small appliances as e.g., phone sets and electric toothbrushes to high power devices as e.g., electric vehicles and other industrial mobility systems. Safety analysis can be performed in the case of small device such as handset antennas and wireless resonant power systems, see e.g., [10–13]. In the case of high power devices as electric vehicles, e.g., [14–20], since the strong near EMFs can induce, important fields in the body of close persons, we require to detect the circumstances where the system can comply with safety atmospheres, see e.g., [21–24]. The exposure to EMFs has different effects in these two cases. As mentioned before these effects are strongly linked to both natures of the EMF and the matter exposed. The field strength and its wave frequency and form characterize the EMF nature while the matter-exposed nature is related to biological properties and geometric characters of different parts and tissues of the body. In the case of wireless communication tools (WCT), the field strength is relatively moderate but the operated frequency is high, radiofrequency (RF), and the exposed body part is mainly the head zone. In this case, the most significant biological effect (BE) is focused on brain. This effect is of two types, thermal and non-thermal. In the case of wireless or inductive power transfer (WPT or IPT), the field strength could be strong with high stray level, the frequency is relatively low and the exposure concerns bodies nearby the device. In these circumstances, the BE regards the induction of different fields in the body, which is limited by international standards [1–3]. Note that, BEs due to EMFs exposure could be investigated in other situations than WCT and WPT such as for example in the case of THz EMFs exposure in wireless communication systems [25] and high voltage transmission lines, see e.g., [26].

Concerning the risk of disturbance of medical devices in healthcare, investigations were devoted to the exposure to the electromagnetic environment of human body on-board devices in general and of piloted therapeutics and interventions. The case of on-board devices involves the static fixed-function case such as wearable sensing devices, e.g., [27–29] and the active devices case such as organ stimulating tools, e.g., [30,31]. The case of piloted operations could be assisted by imaging in particular if it involves displacement or localization. Representative situations in this case are image-guided interventions, as well as image-assisted active drug delivery therapies, e.g., [32–38]. This assistance provides an excellent localization tool improving therapeutic or interventional outcome and allowing precise minimally invasive procedures. The choice of imaging technology follows different criteria depending of the exercised case. The most common biomedical imaging technologies can exert X-rays, ultrasound, magnetism, or radioactive pharmaceuticals. In the last technology, the two most common techniques are scintigraphy and positron emission tomography (PET). The first consists in administering to the patient a small quantity of a radioactive substance emitting gamma rays (or "radioactive tracer"), which attaches itself to the organ or tissue to be explored. The imagers involved in each of these cases are more or less suited to a given situation. These imagers could be used in addition to diagnostic tools, in image-assisted therapy sets or for image-guided interventions as mentioned before. For standard imaging conditions where exposure to the imager is of restricted duration, there are no restraints related to the type of these imagers. Thus, the issue of ionizing radiation implicated in some of these imagers does not inflict any critical restriction. On the other hand, in the occurrence of prolonged exposure to the imager as in the case of image-assisted treatments, only the Magnetic Resonance Imager (MRI) and the Ultrasound Imager (USI) are free of ionizing radiation critical disadvantage [34–38]. Nevertheless, these two imagers undertake particular constraints. The MRI is subject to a protected electromagnetic environment, electromagnetic compatibility (EMC) [39–45] and the USI can only exercise in an ultrasound window (without air or bones).

This contribution aims to analyze and review the effect of, EMFs emitted by energy devices, on BEs in human tissues and on disturbances of medical instruments for healthcare. In the article, the effects of EMFs exposure and their BEs in both cases of wireless telecommunications tools and inductive WPT charging systems are analyzed and assessed. Then, we examine the electromagnetic exposure troubles in the instruments incorporated

in the human body as well as in those used in medical care. The means of evaluating, controlling and adjusting the EMF effects through EMC analysis by numerical modelling are discussed and reviewed.

2. Biological Effects Due to EMFs Exposure

Considering exposure to EMFs, scientific investigates, observational practice and data from patients clearly show the relationships between exposure to EMFs and health problems. These BEs due to exposure to EMFs are obviously related to the nature of such fields.

2.1. Characteristics of EMFs

Exposure to EMFs produces different BEs that depend on the type of the field. EMF involves different characteristics related to the field strength and the frequency range used. The frequencies are divided in static (0 Hz), alternating (1 Hz–10 THz) and specific pulsated fields. The alternating one is often classified as Low (1–300 Hz), Intermediate (300 Hz–100 kHz), Radio and microwave (100 kHz–300 GHz), Terahertz (100 GHz–10 THz).

2.2. Introduction of BEs of Different Types of EMFs

In this section, we will discuss the BEs of the static fields, the alternating frequency fields and the specific pulsated fields (as e.g., MRI pulsed field gradients).

2.2.1. Static Fields

In theory, the safest of the various EMFs is the static field. According to literature, only the presence of ferromagnetic substances in onboard devices or cardiac pacemakers in the exposed subject's body could cause comfort risks linked in particular to contact with a static field of relatively important value, e.g., in the case of the principal magnet in MRI (0.2–10 T).

2.2.2. Alternating Frequency Fields

RF sources act for the most danger to human safety. The specific absorption rate (SAR) operated in these sources could reach in some applications ten W/kg depending on the amplitude of the field and its frequency. For a short interval, this is sufficient to generate a rise in body temperature of 1 °C, which in a healthy subject is completely away of risk and below the limits stated by the international safety references. The higher the SAR and the longer the exposure time, the temperature rise will be more important and dangerous.

Many new technologies, from induction heaters to wireless energy transfer, produce EMF in the intermediate frequency (IF) and the radio frequency (RF) ranges (300 Hz–3 GHz). The effects of these fields on biological organisms, however, have been insufficiently investigated (see Section 5. Discussion). For example, the first generation of several new wireless technology devices was released without any certainty about their health effects, causing new social and medical challenges. Typical applications in this category concern wireless communication tools as mobile smart phones and wireless inductive power transfer systems as battery chargers from small devices to electric vehicles (EV). Details of these applications will be extended later in the paper.

2.2.3. Specific Pulsated Fields

Regarding the case of specific pulsated fields, one may consider the example of MRI pulsed field gradients. The conforming gradient coils are conceived to produce a field gradient (position dependent magnetic field). Proper design of the dimension and contour of the coils is necessary to engender an adjusted and heterogeneous 3D gradient [43]. Due to the growing demand for shorter cycles with bigger temporal and spatial resolutions, the enhancement of modern gradient structures has guided in the recent years to amplify significantly the gradient output (strength and slew rate) that lower imaging time.

Due to the intensification of the source output, one can expect the arrival of unpleasant side effects for the exposed subjects. High efficiency sources cause a fluctuating electric field, which can produce unpleasant peripheral nerve stimulation (PNS) and/or cardiac stimulation [46]. These fields, if of sufficient intensity and interval, can cause PNS with spatially restricted symptomatic sensations of muscle compression, irritation, or astringency. Alternatively, PNS, which can be uncomfortable however if not worrying to the subject, has a border inferior than the intensity estimated for possibly life-alarming cardiac stimulation [46]. Therefore, a high output source could cause harmful biological effects. It is worth mentioning that from the last lines we are in incidence of an optimization defy. Most of clinical researches on PNS are experimental but this could be modeled.

2.2.4. Concluding Remarks on BEs of Different Types of EMFs

The preceding discussion shows that safety awareness of EMF effects can help optimize both the safety and efficiency of the structural process. Industrial systems involving such EMFs are supposed to comply with universal standards allowing restricting the exposure level to meet safety requirements. Hence, the design, the optimization and the verification of these systems are tightly related to such exposure.

2.3. Evaluation of Interaction of EMF and Objects

The evaluation of the effects of EMF on tissues or objects in general can be exercised experimentally or by mathematical modeling. In such evaluation, we need a representation of human body involving a detailed knowledge of the dielectric properties of human tissues at the frequency of operation frequency. For experimental evaluation, due to security issues, such representation (phantom) is built of a physical model that involves the same geometry and matter properties of the considered part of the body. As well, for mathematical modeling evaluation, a numerical phantom is used accounting for geometrical and material proprieties aspects in the numerical representation. Such a phantom corresponds in general to a high-resolution human anatomical model that is compatible with the digital approach used. It is built from a human MRI model (see Section 4.3).

2.4. EMF in Wireless Energy Transfer

The two theories governing wireless energy transfer are Ampère's Law of 1820 and Faraday's Magnetic Induction Principle of 1831. These foundations later enabled Nikola Tesla (1856–1943) to introduce wireless energy transfer for the first time in the 1890s [47–49]. The technology of wireless energy transfer has been first established for transmission of power over long distances using microwave rays [50,51]. Likewise, the notion of wireless power transfer WPT forecasts electric power generation from solar energy in space, through solar-power satellites and microwave power transmission for use on earth [52,53]. It is only recently that near-field close-range inductive WPT (IPT) technology has been widely exploited for charging the batteries of many everyday devices as mobile phones, domestic stuffs, drones, and electrically powered vehicles [14–20]. Inductive power transfer (IPT), inductive coupling, and resonant power transfer, generally refer to wireless power transfer (WPT). These different terms refer to the same process-the contactless transfer of energy from a power source to a load through an air gap. A wireless power transfer system consists of two coils-a transmitter and a receiver.

2.5. BEs Produced by Wireless Devices

Two considerations motivate research efforts on the interactions between wireless structures and the human body. The first is to evaluate the electromagnetic fields provoked in the human body. These fields are magnetic flux density, electric field and current density. Such estimate makes it possible to assess the potential effects on health besides to inspect agreement with the standards defined by the International Commission for the Protection against Non-Ionizing Radiation (ICNIRP) [1,2]. The other aspect is to assess the impact of the input of the wireless device on the radiation levels and thus manage the design and

optimization of systems. Next, we will discuss the BEs due interactions with WCT and IPT devices.

2.5.1. BEs Due to Interaction with WCTs

As mentioned before EMF exposure in RF range is quantified by the SAR. In the case of WCTs, the energy absorption is concentrated near to the head zone of human body and the SAR in this case is generally limited to a value of (0.5–2.0) W/kg. This permits to restrict the temperature rise in the head zone. Note that the SAR limits are 2.0 for the head and body and 4.0 W/kg for the limbs. Details of the SAR and thermal effects [4–9] will be extended later in the paper.

BEs involve in addition to the thermal effect other effects due to EMF for RF and other frequency ranges. These so-called non-thermal effects are potential long-term effects from exposure to slight amounts of EMF (see Section 5 Discussion). These relate to the effects of common sources such as RF radiation emitted by antennas, Wi-Fi access points, smartphones, tablets and Bluetooth devices. As well low frequency (LF) EMF emitted by electrical wiring, lamps and appliances. Similarly, fields due to voltage and current harmonics from electrical wiring, fluorescent lamps and electronic devices.

2.5.2. BEs Due to Interaction with IPT

An important application of IPT concerns recent researches on the development of electric vehicles. In this instance, due to electromagnetic compatibility and energy efficiency, the IPT in EV normally works in inferior frequency scale (from a little kilohertz to about 100 kHz). In this frequency range, exposure investigations to wireless inductive charging structures have not been sufficient so far (see Section 5 Discussion). The assessment of human tissue EMF exposure from IPT requires generally either experimental precise sensing covering the whole elements of the involved scenery or numerical simulation emulating such scenery. This last relates appropriate and sufficient modeling methodologies based on the application of 3D calculations to solve the electromagnetic problem including the IPT set, the vehicle and the human body (in the vehicle or located on the side) see for example [21,54,55]. In this 3D model, the human body can be represented by the equivalent phantom mentioned in (Section 2.3). The global 3D numerical approach encompassing the phantom and the IPT system as well as the vehicle provides an evaluation of human exposure to such system. Electromagnetic exposure assessment should be performed for worst body case configurations.

3. Disturbance of Health Instruments Due to EMF

In this section, we will assess the risk of disruption of medical devices incorporated (into or touching) the body or used in healthcare. This involves two categories: static devices and dynamic therapeutic or interventional devices. The static one involves integrated embedded devices, wearable and removable devices. The second one concerns integrated therapeutic drug delivery as well as interventions and surgeries devices. High precision, accurate localization and minimally invasive operations suggest for the last category image-guided practice.

3.1. Static Devices

We will examine first the case of static devices. Recently, many advances in biocompatible materials have led to the development of implantable devices that enable diagnosis and prediction through small sensors and biomedical devices, dramatically improving the quality and efficiency of healthcare. Another type of static implantable devices that can insure stimulation or activation of an organ such as pacemakers, neuro stimulators or pumps, we call this category active implants [30,31]. Additionally, wearable biosensors and devices that are real-time non-invasive instruments allow continuous monitoring of individuals and thus provide enough information to determine health status or even a preliminary medical diagnosis [27–29]. Additionally, removable and connectable smart

sensing devices that are real-time health monitoring systems for physiological signals closely associated with physical conditions. Such real-time disease monitoring for personalized healthcare involves detecting signals such as heart rate, blood pressure, and respiratory rate to extract clinically relevant information [56–58]. Additionally, implantable devices, wearable biosensors, and smart removable devices allow healthcare providers to monitor the physiological characteristics of patients after therapy or treatment [59,60]. These three types of devices correspond to on-board autonomous static devices involving active implants such as pacemakers or pumps.

Note that commitments from health care organizations increase support for integrated and connected personalized care to support the delivery of health services. Thus, using Hospital at home and connected ambulance paradigms instead of face-to-face care. The implantable, portable and removable technologies mentioned are part of this personalized care.

The protection of these static devices against electromagnetic fields can be ensured in different ways. Thus by avoiding ferromagnetic parts in their construction, by shielding, or by avoiding exposing them to strong EMFs such as the insertion in the DC magnet of an MRI.

3.2. Image-Guided Therapeutic and Interventional Devices

The case of dynamic therapeutic devices concerns mainly, image-guided therapies. These are integrated therapies that expending locally constrained dynamic active drug delivery tools. Such therapeutic configurations could practice active implant supports. In the case of image-guided interventions, robotic surgical arms or needles can be used assisted by the imager. These two cases, the dynamic active implant and the surgical robot perform a minimally invasive process. They are supposed to be interconnected to the imager via a two-way sense-control link. Such a link involves image processing, control management and information matching. Figure 1 shows an interactive real-time autonomous image guided drug release system. Besides the minimally invasive advantage, we can improve the smoothness of imaging by using non-ionizing devices that use universal sensing. As discussed before the MRI seems to be the suitable candidate. The only restriction on this imager, which uses different fields, is its sensitivity to outer EM noise causing severe operational disturbances. This requires avoiding external EMF radiations and minimizing ferromagnetic and conductive materials in the imager landscape. Thus, the imager must be shielded and the auxiliaries must be constructed of compatible materials and powered by shielded connections. These auxiliaries involve in the present case robotic arms and dynamic implant supports as well as their actuating devices. The control of the mentioned operational disturbances and the compatibility of materials can be achieved by means of EMC analysis.

3.3. EMC Analysis in MRI

The MRI imaging system uses three devices producing EMFs. A static magnetic field magnet, magnetic field gradient coils and a source of radio frequency pulses. The constant magnetic field must be uniform and the position-dependent field gradient must be regulated and homogenous. These two fields require compensation and rectification to meet the typical functioning of the imager. The RF source has a frequency identical to that of Larmor of the protons, which is dependent on the value of the static field and given by 42.5 MHz per tesla. The RF EMF is the most vulnerable of the three involved fields. The BEs of these fields have been shortly reviewed concerning the gradient field [46] in Section 2.2., more general review could be found in [61].

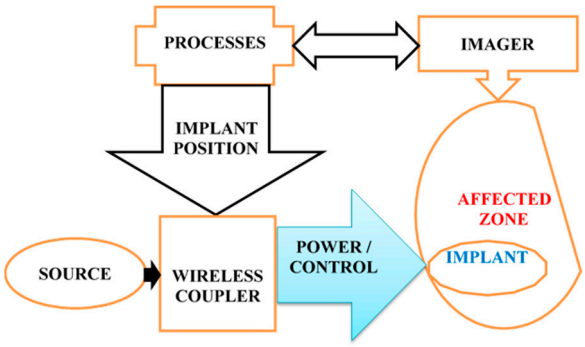

Figure 1. Collaborative simultaneous self-ruling image guided drug release system.

The MRI apparatus as mentioned before is very allergic to electromagnetic noise, which can generate image degrading. The incorporation of magnetic or conductive components into the environment close to the MRI participates considerably to this noise. The definition of MRI compatibility is related to such an environment.

Therefore, in image-assisted processes for integrated therapies as well as interventions, the devices involved must use MR-compatible materials [39–45] and must use MR-compatible actuation [62–68].

EMC analysis targets to control the effect of hosting in the MRI environment, different materials and structures, on the imaging performance. Such analysis could be generally exercised experimentally or with the help of mathematical modeling. The experimental issue to control the compatibility uses high precision-networked sensed measurements covering the involved scenery. In the case of MRI scenery, this task is very complicated and represent a serious risk for the imager installation due to the introduction of foreign matters. Therefore, the modeling focus through numerical simulation of the functioning of the imager seems more adequate for verifying the compatibility. This will be detailed in the next section—Modeling of EMF.

4. Modeling of EMF Exposure and EMC

In order to model the interactions between systems emitting EMF and the human body or health instruments, we need to solve locally the governing equations. Three questions generally motivate the analyses: estimating the fields induced in the human body, assessing the danger of disturbance of medical devices (integrated or not) through EMC computations and the last issue regarding the design, optimization and monitoring of the emitting systems and exposed devices.

4.1. EMF Equation System

The system of EMF equations that is based on Maxwell equations can be expressed mathematically in diverse forms depending on the problem under consideration. Moreover, the numerical treatment necessary for locally solving the problem as well as the nature of the used discretization elements influence the choice of such form. One of the most familiar is the fundamental full-wave electromagnetic formulation given by:

$$\nabla \times \mathbf{H} = \mathbf{J} \tag{1}$$

$$\mathbf{J} = \sigma\, \mathbf{E} + j\, \omega\, \mathbf{D} + \mathbf{J_e} \tag{2}$$

$$\mathbf{E} = -\nabla\, V - j\, \omega\, \mathbf{A} \tag{3}$$

$$\mathbf{B} = \nabla \times \mathbf{A} \tag{4}$$

where **H** and **E** are the magnetic and electric fields, **B** and **D** are the magnetic and electric inductions, **A** and V are the magnetic vector and electric scalar potentials. **J** and $\mathbf{J_e}$ are the total and source current densities, σ is the electric conductivity and ω is the frequency pulsation. The symbol ∇ is a vector of partial derivative operators, and its three possible

implications are gradient (product with a scalar field), divergence and curl (dot and cross products respectively with a vector field).

The magnetic and electric comportment laws respectively between **B/H** and **D/E** are represented by the permeability μ and the permittivity ε.

The solution of Equations (1)–(4) allows to determine in a system the EMFs for a given frequency pulsation taking into account the behaviors of magnetic materials via permeability, the eddy currents in electrical conductors across electrical conductivity and the displacement currents in dielectrics thru permittivity.

The induced EMF in the body tissues can be obtained from the solution of (1)–(4). As well, the SAR and its thermal effect can be computed using the fields resulting from such solution (see the next section). Also, the EMC analysis checking the perturbations due to EMF exposers of instruments (embedded or not) can be verified from such solution.

4.2. SAR and Thermal Effect

As mentioned before SAR quantifies the energy absorbed in an element of the tissue. It can represented by:

$$SAR = P/\rho = \sigma E^2/(2\,\rho) \quad (5)$$

where, SAR is specific absorption rate in (W/kg). P is the power loss density in (W/m^3), ρ the density of tissue (kg/m^3), E the electric field strength in (V/m), σ the conductivity (S/m). Note that the conductivity is matter and frequency dependent. In human tissue, the conductivity is generally constant with augmenting frequency until megahertz frequencies, and then it increases, often in an approximately linear manner.

The RF EMFs exposed object concerns the human head and body, we have to control the security conditions of emitting devices [4–9]. The temperature distributions in tissue exposed to these fields can be determined by solving the equation of bio-heat transfer [69]. Primarily, the SAR distribution due to exposure to external source is calculated, and then geometrical parameters and thermal properties are included in model.

In general, the amount of heat quantity absorbed by a tissue or more generally of a lossy dielectric can be given as:

$$\Delta Q = c\,m\,\Delta T \quad (6)$$

where Q is the heat energy absorbed or dissipated in joule (J), m is the mass of the substance (kg), ΔT is the change in substance temperature (°C), c is the specific heat of the substance (the heat required to change a substance unit mass by one degree) in J/(kg °C).

The power absorbed per unit mass of substance exposed to RF radiation (SAR) in W/kg, which corresponds to the time derivative of the energy in J absorbed per unit mass in kg of substance can be given for an exposure time Δ t in (s) by:

$$SAR = \Delta Q/(m\,\Delta t) = c\,\Delta T/\Delta t = \sigma E^2/(2\,\rho) \quad (7)$$

This expression implies that the SAR value of substance depends on the induced electric field intensity, the exposure time, and the tissue electrical-thermal properties. The energy absorbed by the substance is converted to thermal energy causing to increase the temperature.

The temperature rise ΔT due to power dissipated by an electric field interacting with a lossy dielectric material specimen given for an exposure time Δ t is given by:

$$\Delta T = \sigma E^2\,\Delta t/(2\,c\,\rho) \quad (8)$$

Penne's bio-heat equation [69] is usually used to determine heat transfer in living tissues:

$$c\,\rho\,\partial T/\partial t = \nabla\,(k\,\nabla T) + q_{ex} + q_{met} - c_b\,W_b\,(T - T_b) \quad (9)$$

In bio-heat equation, SAR is associated as follows:

$$c\,\rho\,\partial T/\partial t = \nabla\,(k\,\nabla T) + \rho\,(SAR) + q_{met} - c_b\,\rho_b\,\omega_b\,(T - T_b) \quad (10)$$

where k is tissue thermal conductivity, T local temperature of tissue, q_{ex} and q_{met} are respectively the exposure heat source and basal metabolic heat source in W/m^3, c_b and W_b are respectively blood specific heat in J/(kg °C) and perfusion coefficient in $kg/(m^3.s)$. In addition, ρ_b is blood density in kg/m^3, ω_b is blood perfusion rate (1/s), T_b blood temperature. $\nabla\,(k\,\nabla T)$ represents simple heat equation in differential form and $\rho\,(SAR)$ represents the influence of electromagnetic energy absorbed in the human tissues.

Thermal behavior in tissues due to EMF exposure, for a given frequency and a denoted duration, is governed by Equations (1)–(5) and (10). The EMF equations and the heat transfer equation must be solved in a coupled fashion. Due to slow thermal time behavior compared to fast EM time behavior, i.e., very high thermal time constant versus very small for EM, we can use weak coupling. Thus, the two systems of equations are solved successively [9,70,71].

4.3. Body Models

Substantial research has gone into building models of human bodies. In general, the use of numerical simulations to calculate electromagnetic fields in human body models necessitates appropriate computer models of the body and complete data of the dielectric properties of tissues at the operating frequency. The models are generally categorized into homogeneous and non-homogeneous. For the first, the dielectric properties of the human body are habitually designated as a 2/3 equivalent muscle model [72]. For non-homogeneous ones, layered tissue phantom models are centered on data acquired from MRI, computed tomography and numerical imaging procedures, offering tissue outline precision on the order of mm [73,74]. Figure 2 shows a structural body model and its diverse tissues and organs. Such a high-resolution human model is harmonious with the numerical approaches used for the determination of induced fields in human's tissues. The dielectric properties of biological tissues are widely tabulated in [75,76]. A detailed picture of accessible measurement information for dielectric permittivity and electrical conductivity for an indicated frequency is provided in [76].

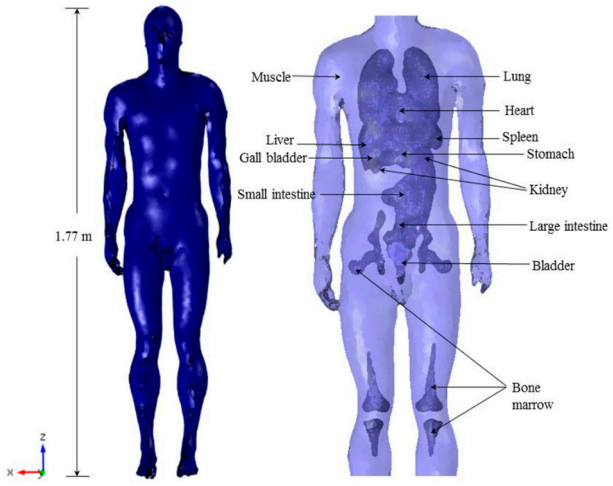

Figure 2. High-resolution anatomical entire body model and its various tissues and organs.

4.4. Solution Approach

The Equations (1)–(4) relative to EMF as well as (5) and (10) regards SAR and its thermal effect must be solved locally in the 3D domain signified by the phantom conforming to the tissue of the body part concerned. This could be done by using a solution in

discretized reduced elements resulting from the cutting of the studied 3D domain. Different methods can be used such as finite differences or finite elements [77–85].

The output of the calculations are the local values of the various fields and their distributions in the 3D domain. These also make it possible to determine global quantities such as energy, power, losses, etc. In addition, consistency with the thresholds linked to health issues and EMC constraints can be checked from field values.

For example, consider the case of EM exposure of IPT involved in EV. Figure 3 shows an example of the distributions of induced fields in human body in the case of exposure to an IPT in EV. The corresponding configuration involves the human body horizontally laying on the ground beside the vehicle, the IPT coils with ferrites and the EV chassis [54]. The human body corresponds to the high-resolution human anatomical model, compatible with the used numerical approach, shown in Figure 2. The related results are in agreement with international safety guidelines (27 µT for the magnetic induction B and 4.05 V/m for electric field E).

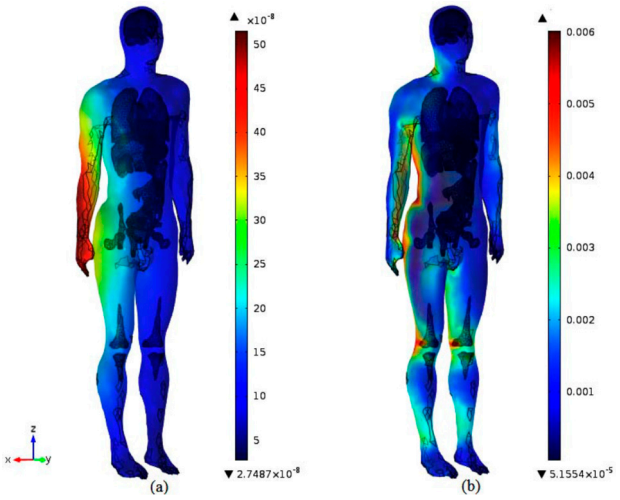

Figure 3. Distribution of induced fields in the human body, by an IPT under EV, for the configuration of horizontal, ground lying body beside the EV. (**a**) Magnitude of magnetic flux density B (T), (**b**) Magnitude of electric E-field (V/m).

4.5. Design, Optimization and Monitoring of Interacting EMF Concerns

The reduction of the effects of EMFs emitted by energy devices could be achieved in two ways. The first is related to the shielding technologies used both on the exposed side (for devices and instruments) and on the emitting side. The second relates to the adaptation of the structure, materials and control of the emitting devices by using computer aided engineering (CAE) tools. Moreover, the monitoring of these effects in the exposed devices could be exercised by EMC analysis.

4.5.1. Shielding Technologies

These technologies generally use materials that absorb or reflect the incident electromagnetic wave to prevent it from passing through the shielding layer. The EM interference (EMI) shielding coatings, layers and devices that can withstand harmful electromagnetic pollution are essential for the normal operation of medical devices and for ensuring human health and safety. Generally, electromagnetic fields consist of magnetic fields and electric fields perpendicular to each other. In this respect, EMI shielding mechanisms can be mainly classified into electrical, magnetic, and electrical-magnetic coupled EMI shielding. Note that the electric and magnetic fields of the RF waves that characterize the radiation asset are interdependent; thus, the shielding of one of them can lead to the mitigation of the other. This is the central cause why habitual EMI shielding materials are frequently conductive materials. Function of the different necessities, materials could be split into cloth, rubbers, adhesives and coatings. The flexibility, process ability, sealing ability and stability indicate

such material form. Due to the increasing EM pollution, investigations in EMI shielding materials have been very active in recent years; see e.g., [86–97].

4.5.2. CAE and EMC Supervising

The calculations described in the last section make it possible to reduce the effects of exposure to EMF either by optimizing the source structures or by improving the protection of the exposed objects. This involves the use of CAE and optimization tools by iterative procedure involving the solution of the equations described in the previous section. These tools aim to manage the geometric and material properties of the structures concerned as well as the behavior control thru consistency with the different thresholds. This consistency can be checked from the supervision of adjusted field values concerning the associated threshold. By following such a strategy, the various devices used by humans as WCT or operating in close proximity as IPT can be designed to reduce emitted EMF respecting threshold regarding BE in tissue, see e.g., [98,99].

In addition, EMF disturbances of medical devices combined with the human body or used in healthcare can be monitored by EMC analysis. Thus, the effect of the introduction of external sources or materials into a defined perimeter of the device can be evaluated and therefore the acceptability of such an introduction. Such EMC analysis can be performed for embedded, portable, and removable medical devices as well as for integrated therapeutic drug delivery and interventional devices. Moreover, the above discussed shielding structures can be formulated based on the mentioned CAE tools and their shielding efficacy can be controlled by EMC analysis.

4.5.3. Case of EMC Monitoring in MRI

Consider for example the case of disturbances in the distribution of the RF magnetic field inside the tunnel of an MRI, which are generally caused by external EMFs or the insertion of magnetic or conductive materials into the atmosphere of the imager. In MRI-guided therapies and interventions, only tools and actuation devices made of non-magnetic and non-conductive materials are permitted. Piezoelectric material is normally allowed and actuators constructed of such material can generally be used. These actuators use electrodes (very thin conductive layers) permitting the excitation of the piezoelectric material. The monitoring of the disturbance due to the introduction of piezoelectric and conductive materials showed that only the conductor is faulty [45]. Moreover, in the same work, the case of a simple structure of piezo material coated with two electrodes of conductive thin films was supervised by EMC analysis. Figure 4 shows the distribution of the MRI RF magnetic field (directed vertically) in the axial section of the birdcage inside the MRI tunnel for the reference case: no material. In Figure 5, the case of a cubic form piezoelectric material ($\mu_r = 1$, $\varepsilon_r = [450\ 990\ 990]$, $\sigma = 0$ S/m) coated on two opposite faces by conductor thin electrodes ($\mu_r = 1$, $\varepsilon_r = 1$, $\sigma = 3.77 \times 10^7$ S/m) is considered (see Figure 5a). The figure shows the distribution of the field in the two cases where the electrodes are perpendicular (Figure 5b) and parallel (Figure 5c) to the direction of the field.

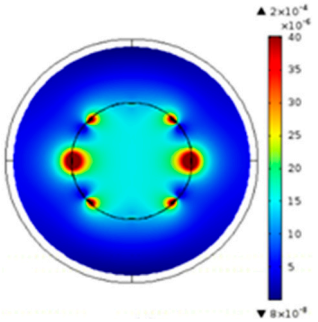

Figure 4. MRI RF magnetic field (vertically directed) distribution in the reference case: no material in the birdcage within the MRI tunnel [45].

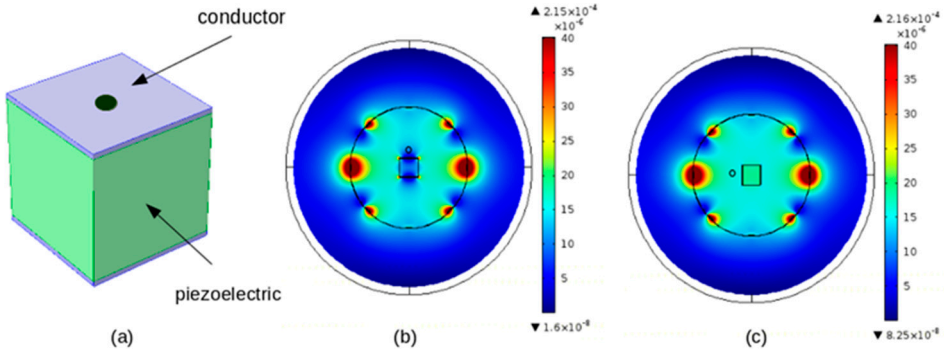

Figure 5. MRI RF magnetic field distribution in the case of the introduction of a piezoelectric with electrodes (**a**) material configuration (**b**) field distribution with electrodes perpendicular to the field (**c**) field distribution with electrodes parallel to the field [45].

Note that, the piezoelectric material is expected not to disturb the field and that the direction of the thin conductors with respect to the field plays an important role, this is related to the importance of the surface of the conductor perpendicular to the direction of the field. In Figure 5 we see that only the conductors (with electrodes perpendicular to the field) disturb the field and that the impact of the conductors can be significantly reduced when they are parallel to the field. It may be noted that the field distributions in Figures 4 and 5 are obtained for the same source condition and give a behavioral indication. Moreover, it is supposed that the other two MRI fields, the DC and gradient, are compensated and shielded.

The last example of EMC Monitoring in MRI, illustrates a methodology for analyzing and controlling possible disturbances in image-guided interventions or implants.

5. Discussion

In this contribution, the followed analysis and review of the impact of EMFs emitted by energy devices have shown that such an impact cannot be neglected and must be predicted and controlled to reduce its effects. At this stage, various subjects are worth commenting on:

- Several actors are affected by the problems analyzed in this work and must remain attentive to the relevant issues, each in their sector. These actors mainly concern the public health sector, manufacturers of electromagnetic energy devices, manufacturers of medical instruments, developers of digital models and of course patients. More categories that are general, involve researchers, educators, and consulting engineers in the electromagnetic energy industry. The issues concern the design and shielding of electromagnetic energy tools, as well as the compensation, protection and proper use of medical instruments. All of these aspects must meet safety standards.
- Maladies that are chronic or associated with unknown symptoms are on the increase and medicine is gradually confronted with health problems with unknown causes. In addition to general societal chronic stress, chemical exposures at home, at work and during outdoor activities are sources of environmental stress that deserve medical and health care consideration. The present contribution reinforce the necessity to consider the exposure to EMFs. In addition, long-term exposure to certain electromagnetic fields is widely recognized as a risk issue for diseases such as specific cancers, Alzheimer's disease and male infertility [100]. Due to this, different thresholds have been established by safety standards. Moreover, the effects of EMFs on biological organisms for frequency ranges involved in common applications and in particular, the so-called non-thermal effects which are potential long-term effects of exposure to low amounts of EMF, have not been sufficiently studied [100].
- In this work, we considered only the BEs due to EMFs that are recognized by the scientific medical community. Actually, health authorities are increasingly recognizing electromagnetic hypersensitivity (EHS) or idiopathic environmental intolerance (IEI)

due to mainly RF EMF. Subjects undergoing EHS show symptoms even when the level of this field is small enough not to produce noticeable BEs. At first, these symptoms occur only sporadically, but later, over time, they can become more pronounced and stronger. Even though these symptoms are real, the scientific medical community does not recognize EHS as a disease and there is no scientific evidence of a causal link with EMF exposure. Several investigations have been carried out to understand this paradoxical situation, e.g., [101–107]. By reviewing the literature, we come to the following inference: the symptoms are real and present in EMF-exposed subjects, even though there is no evidence linking such low exposure to biological effects that exhibit such symptoms. These symptoms are therefore linked to the exposure, but the latter could not be responsible for the biological effects causing these symptoms. Thus, the exposure indirectly induces via an unknown link the effects causing the symptoms. This thesis of the unknown link is evoked in the literature in the form of phobia or anxiety, e.g., [101]. Due to this difficult state, and pending further research, EHS could reasonably be treated clinically as a chronic multisystem disease, recognizing that the primary cause remains the EMF atmosphere.

6. Conclusions

This contribution carried out an assessment of the impact of EMFs emitted by energy devices, on BEs in human tissues and on the perturbations of medical instruments for health care. The consequences of exposure to EMFs and their BEs in both cases of wireless telecommunications tools and inductive WPT charging systems have been analyzed and evaluated. Then, the perturbations of electromagnetic exposure in instruments incorporated in the human body as well as in those used in medical care were examined. Methods for evaluating, controlling and adjusting EMF effects via EMC analysis by numerical modeling were discussed and reviewed. In conclusion, this contribution illustrated the next important points:

- The analysis carried out argues in favor of the importance of predictive modeling of biological effects in human tissues due to emitted EMFs. The predicted values of the fields induced in the digital phantom models make it possible to control the emitting devices and to propose the reduction of their negative effects by optimizing their structure, their material constitution and their shielding efficiency.
- In the case of disturbances of medical tools by emitted EMFs, prediction plays a role not only in the control and optimization of emitting devices but also in the protection of exposed instruments by effective shielding. In addition, predictive modeling via EMC analysis has shown valuable efficiency regarding the monitoring and verification of conditions allowing the acceptability of the introduction of external sources or materials into or near the medical tool such as MRI.
- This article has described a non-exhaustive selection of recent advances developed for the impact of electromagnetic fields emitted by electromagnetic energy devices. Particular attention has been paid to wireless communication and energy transfer tools as well as the monitoring of medical tools. The advances described have widened the field of phenomena that can be explored and have made it possible to generalize the study to a variety of devices that can interface with health.

Funding: This research received no external funding.

Institutional Review Board Statement: Not applicable.

Informed Consent Statement: Not applicable.

Data Availability Statement: Not applicable.

Conflicts of Interest: The author declare no conflict of interest.

References

1. International Commission on Non-Ionizing Radiation Protection. Guide-lines for limiting exposure to time-varying electric and magnetic fields for low frequencies (1 Hz–100 kHz). *Health Phys.* **2010**, *99*, 818–836. [CrossRef] [PubMed]
2. International Commission on Non-Ionizing Radiation Protection. Guidelines for limiting exposure to electromagnetic fields (100 kHz to 300 GHz). *Health Phys.* **2020**, *118*, 483–524. [CrossRef] [PubMed]
3. *IEEE Standard C95.1-2019*; IEEE Standard for Safety Levels With Respect to Human Exposure to Electric, Magnetic, and Electromagnetic Fields, 0 Hz to 300 GHz. IEEE Standards Association: Piscataway, NJ, USA, 2019. [CrossRef]
4. Joshi, M.S.; Joshi, G.R. Analysis of SAR induced in Human Head due to the exposure of Non-ionizing Radiation. *Int. J. Eng. Res. Technol. (IJERT)* **2016**, *5*, 364–367. [CrossRef]
5. Sallomi, A.H.; Hashim, S.A.; Wali, M.H. SAR and thermal effect prediction in human head exposed to cell phone radiations. *Sci. Int.* **2018**, *30*, 653–656.
6. Hamed, T.; Maqsood, M. SAR Calculation & Temperature Response of Human Body Exposure to Electromagnetic Radiations at 28, 40 and 60 GHz mm Wave Frequencies. *Prog. Electromagn. Res. M* **2018**, *73*, 47–59. [CrossRef]
7. Baker-Jarvis, J.; Kim, S. The Interaction of Radio-Frequency Fields With Dielectric Materials at Macroscopic to Mesoscopic Scales. *J. Res. Natl. Inst. Stand. Technol.* **2012**, *117*, 1–60. [CrossRef] [PubMed]
8. Laakso, I.; Hirata, A. Modelling the SAR and thermoregulatory response during far-field RF exposure. In Proceedings of the 2012 Asia-Pacific Symposium on Electromagnetic Compatibility, Singapore, 21–24 May 2012; pp. 729–732. [CrossRef]
9. Bernardi, P.; Cavagnaro, M.; Pisa, S.; Piuzzi, E. Specific absorption rate and temperature elevation in a subject exposed in the far-field of radio-frequency sources operating in the 10–900-MHz range. *IEEE Trans. Biomed. Eng.* **2003**, *50*, 295–304. [CrossRef]
10. Okoniewski, M.; Stuchly, M.A. A study of the handset antenna and human body interaction. *IEEE Trans. Microw. Theory Tech.* **1996**, *44*, 1855–1864. [CrossRef]
11. Shiba, K.; Higaki, N. Analysis of SAR and current density in human tissue surrounding an energy transmitting coil for a wireless capsule endoscope. In Proceedings of the 2009 20th International Zurich Symposium on Electromagnetic Compatibility, Zurich, Switzerland, 12–16 January 2009; pp. 321–324. [CrossRef]
12. Christ, A.; Douglas, M.G.; Roman, J.M.; Cooper, E.B.; Sample, A.P.; Waters, B.H.; Smith, J.R.; Kuster, N. Evaluation of wireless resonant power transfer systems with human electromagnetic exposure limits. *IEEE Trans. Electromagn. Compat.* **2013**, *55*, 265–274. [CrossRef]
13. Lin, J.C. Safety of Wireless Power Transfer. *IEEE Access* **2021**, *9*, 125342–125347. [CrossRef]
14. Covic, G.A.; Boys, J.T. Trends in Inductive Power Transfer for Transportation Applications. *IEEE J. Emerg. Sel. Top. Power Electron.* **2013**, *1*, 28–41. [CrossRef]
15. Hutchinson, L.; Waterson, B.; Anvari, B.; Naberezhnykh, D. Potential of wireless power transfer for dynamic charging of electric vehicles. *IET Intell. Transp. Syst.* **2019**, *13*, 3–12. [CrossRef]
16. Ibrahim, M.; Bernard, L.; Pichon, L.; Razek, A.; Houivet, J.; Cayol, O. Advanced modeling of a 2-kw series–series resonating inductive charger for real electric vehicle. *IEEE Trans. Veh. Technol.* **2015**, *64*, 421–430. [CrossRef]
17. Cirimele, V.; Diana, M.; Freschi, F.; Mitolo, M. Inductive Power Transfer for Automotive Applications: State-of-the-Art and Future Trends. *IEEE Trans. Ind. Appl.* **2018**, *54*, 4069–4079. [CrossRef]
18. Razek, A. Review of Contactless Energy Transfer Concept Applied to Inductive Power Transfer Systems in Electric Vehicles. *Appl. Sci.* **2021**, *11*, 3221. [CrossRef]
19. Ibrahim, M.; Bernard, L.; Pichon, L.; Laboure, E.; Razek, A.; Cayol, O.; Ladas, D.; Irving, J. Inductive Charger for Electric Vehicle: Advanced Modeling and Interoperability Analysis. *IEEE Trans. Power Electron.* **2016**, *31*, 8096–8114. [CrossRef]
20. Cirimele, V.; Diana, M.; Bellotti, F.; Berta, R.; El Sayed, N.; Kobeissi, A.; Guglielmi, P.; Ruffo, R.; Khalilian, M.; La Ganga, A.; et al. The Fabric ICT Platform for Managing Wireless Dynamic Charging Road Lanes. *IEEE Trans. Veh. Technol.* **2020**, *69*, 2501–2512. [CrossRef]
21. Ding, P.; Bernard, L.; Pichon, L.; Razek, A. Evaluation of Electromagnetic Fields in Human Body Exposed to Wireless Inductive Charging System. *IEEE Trans. Magn.* **2014**, *50*, 1037–1040. [CrossRef]
22. Wen, F.; Huang, X. Human Exposure to Electromagnetic Fields from Parallel Wireless Power Transfer Systems. *Int. J. Environ. Res. Public Health* **2017**, *14*, 157. [CrossRef]
23. Wang, Q.; Li, W.; Kang, J.; Wang, Y. Electromagnetic Safety Evaluation and Protection Methods for a Wireless Charging System in an Electric Vehicle. *IEEE Trans. Electromagn. Compat.* **2019**, *61*, 1913–1925. [CrossRef]
24. Cirimele, V.; Freschi, F.; Giaccone, L.; Pichon, L.; Repetto, M. Human Exposure Assessment in Dynamic Inductive Power Transfer for Automotive Applications. *IEEE Trans. Magn.* **2017**, *53*, 1–4. [CrossRef]
25. Spathmann, O.; Zang, M.; Streckert, J.; Hansen, V.; Saviz, M.; Fiedler, T.M.; Statnikov, K.; Pfeiffer, U.R.; Clemens, M. Numerical Computation of Temperature Elevation in Human Skin Due to Electromagnetic Exposure in the THz Frequency Range. *IEEE Trans. Terahertz Sci. Technol.* **2015**, *5*, 978–989. [CrossRef]
26. Gonos, J.; Kladas, A.; Labridis, D.; Mikropoulos, P.; Koulouridis, S.; Pyrgioti, E.; Kyriacou, G.; Safigianni, A. Environmental Impact Analysis of Electric Power Lines. In Proceedings of the 2018 IEEE International Conference on Environment and Electrical Engineering and 2018 IEEE Industrial and Commercial Power Systems Europe (EEEIC/I CPS Europe), Palermo, Italy, 12–15 June 2018; pp. 1–5. [CrossRef]

27. Guk, K.; Han, G.; Lim, J.; Jeong, K.; Kang, T.; Lim, E.-K.; Jung, J. Evolution of Wearable Devices with Real-Time Disease Monitoring for Personalized Healthcare. *Nanomaterials* **2019**, *9*, 813. [CrossRef] [PubMed]
28. Xin, Y.; Liu, T.; Sun, H.; Xu, Y.; Zhu, J.; Qian, C.; Lin, T. Recent progress on the wearable devices based on piezoelectric sensors. *Ferroelectrics* **2018**, *531*, 102–113. [CrossRef]
29. Yetisen, A.K.; Martinez-Hurtado, J.L.; Ünal, B.; Khademhosseini, A.; Butt, H. Wearables in Medicine. *Adv. Mater.* **2018**, *30*, 1706910. [CrossRef] [PubMed]
30. Bernardi, P.; Cavagnaro, M.; Pisa, S.; Piuzzi, E. Safety aspects of magnetic resonance imaging for pacemaker holders. In Proceedings of the 2009 International Conference on Electromagnetics in Advanced Applications, Turin, Italy, 14–18 September 2009; pp. 869–872. [CrossRef]
31. Thotahewa, K.M.S.; Redouté, J.; Yuce, M.R. Electromagnetic and thermal effects of IR-UWB wireless implant systems on the human head. In Proceedings of the 2013 35th Annual International Conference of the IEEE Engineering in Medicine and Biology Society (EMBC), Osaka, Japan, 3–7 July 2013; pp. 5179–5182. [CrossRef]
32. Kovács, A.; Bischoff, P.; Haddad, H.; Kovács, G.; Schaefer, A.; Zhou, W.; Pinkawa, M. Personalized Image-Guided Therapies for Local Malignencies: Interdisciplinary Options for Interventional Radiology and Interventional Radiotherapy. *Front. Oncol.* **2021**, *11*, 616058. [CrossRef] [PubMed]
33. Zhao, J.; Zhi, Z.; Zhang, H.; Zhao, J.; Di, Y.; Xu, K.; Ma, C.; Liu, Z.; Sui, A.; Wang, J. Efficacy and safety of CT guided 125I brachytherapy in elderly patients with non small cell lung cancer. *Oncol. Lett.* **2020**, *20*, 183–192. [CrossRef]
34. Park, B.K. Ultrasound-guided genitourinary interventions: Principles and techniques. *Ultrasonography* **2017**, *36*, 336–348. [CrossRef]
35. Pinto, P.A.; Chung, P.H.; Rastinehad, A.R.; Baccala, A.A.; Kruecker, J.; Benjamin, C.J.; Xu, S.; Yan, P.; Kadoury, S.; Chua, C. Magnetic resonance imaging/ultrasound fusion guided prostate biopsy improves cancer detection following transrectal ultrasound biopsy and correlates with multiparametric magnetic resonance imaging. *J. Urol.* **2011**, *186*, 1281–1285. [CrossRef]
36. Fiard, G.; Hohn, N.; Descotes, J.L.; Rambeaud, J.J.; Troccaz, J.; Long, J.A. Targeted MRI-guided prostate biopsies for the detection of prostate cancer: Initial clinical experience with real-time 3-dimensional transrectal ultrasound guidance and magnetic resonance/transrectal ultrasound image fusion. *Urology* **2013**, *81*, 1372–1378. [CrossRef]
37. Veltri, A.; Garetto, I.; Pagano, E.; Tosetti, I.; Sacchetto, P.; Fava, C. Percutaneous RF thermal ablation of renal tumors: Is US guidance really less favorable than other imaging guidance techniques? *Cardiovasc. Interv. Radiol.* **2009**, *32*, 76–85. [CrossRef] [PubMed]
38. Bassignani, M.; Moore, Y.; Watson, L.; Theodorescu, D. Pilot experience with real-time ultrasound guided percutaneous renal mass cryoablation. *J. Urol.* **2004**, *171*, 1620–1623. [CrossRef] [PubMed]
39. Chinzei, K.; Kikinis, R.; Jolesz, F.A. MR compatibility of mechatronic devices: Design criteria. In Proceedings of the International Conference on Medical Image Computing and Computer-Assisted Intervention, Cambridge, UK, 19–22 September 1999; pp. 1020–1030.
40. Tsekos, N.V.; Khanicheh, A.; Christoforou, E.; Mavroidis, C. Magnetic resonance-compatible robotic and mechatronics systems for image guided interventions and rehabilitation: A Review Study. *Annu. Rev. Biomed. Eng.* **2007**, *9*, 351–387. [CrossRef] [PubMed]
41. Khairi, R.; Razek, A.; Bernard, L.; Corcolle, R.; Bernard, Y.; Pichon, L.; Poirier-Quinot, M.; Ginefri, J.C. EMC analysis of MRI environment in view of Optimized performance and cost of image guided interventions. *Int. J. Appl. Electromag. Mech.* **2016**, *51*, S67–S74. [CrossRef]
42. Boutry, C. Biodegradable Passive Resonant Circuits for Wireless Implant Applications. Ph.D. Thesis, ETH Zurich, Zurich, Switzerland, 2012.
43. Razek, A. Towards an image-guided restricted drug release in friendly implanted therapeutics. *Eur. Phys. J. Appl. Phys.* **2018**, *82*, 31401. [CrossRef]
44. Hsu, Y.H.; Chen, D.W.; Tai, C.D.; Chou, Y.C.; Liu, S.J.; Ueng, S.W.; Chan, E.C. Biodegradable drug-eluting nanofiber-enveloped implants for sustained release of high bactericidal concentrations of vancomycin and ceftazidime: In vitro and in vivo studies. *Int. J. Nanomed.* **2014**, *9*, 4347–4355. [CrossRef]
45. Razek, A. Assessment of Supervised Drug Release in Cordial Embedded Therapeutics. *Athens J. Technol. Eng.* **2019**, *6*, 77–91. [CrossRef]
46. Den Boer, J.A.; Bourland, J.D.; Nyenhuis, J.A.; Ham, C.L.; Engels, J.M.; Hebrank, F.X.; Frese, G.; Schaefer, D.J. Comparison of the threshold for peripheral nerve stimulation during gradient switching in whole body MR systems. *J. Magn. Reson. Imaging* **2002**, *15*, 520–525. [CrossRef]
47. Tesla, N. System of Transmission of Electrical Energy. U.S. Patents 645576, 20 March 1900.
48. Tesla, N. The transmission of electrical energy without wires. *Electr. World Eng.* **1904**, *1*, 429–431.
49. Tesla, N. Apparatus for Transmitting Electrical Energy. U.S. Patents 1119732, 1 December 1914.
50. Brown, W.C. A survey of the elements of power transmission by microwave beam. *IRE Int. Conv. Rec.* **1961**, *9*, 93.
51. Brown, W.C. The history of power transmission by radio waves. *IEEE Trans. Microw. Theory Techn.* **1984**, *32*, 1230–1242. [CrossRef]
52. Glaser, P.E. Power from the sun: Its future. *Science* **1968**, *162*, 857–861. [CrossRef] [PubMed]
53. Brown, W.C. Satellite power stations: A new source of energy? *IEEE Spectr.* **1973**, *10*, 38–47. [CrossRef]
54. Razek, A.; Pichon, L.; Kameni, A.; Makong, L.; Rasm, S. Evaluation of Human Exposure owing to Wireless Power Transfer Systems in Electric Vehicles. *Athens J. Technol. Eng.* **2019**, *6*, 239–258. [CrossRef]

55. Cimala, C.; Clemens, M.; Streckert, J.; Schmuelling, B. Simulation of Inductive Power Transfer Systems Exposing a Human Body with a Coupled Scaled-Frequency Approach. *IEEE Trans. Magn.* **2017**, *53*, 1. [CrossRef]
56. Pantelopoulos, A.; Bourbakis, N.G. A survey on wearable sensor-based systems for health monitoring and prognosis. *IEEE Trans. Syst. Manand Cybern. Part C* **2010**, *40*, 1–12. [CrossRef]
57. Chan, M.; Esteve, D.; Fourniols, J.Y.; Escriba, C.; Campo, E. Smart wearable systems: Current status and future challenges. *Artif. Intell. Med.* **2012**, *56*, 137–156. [CrossRef]
58. Kim, J.; Campbell, A.S.; de Ávila, B.E.; Wang, J. Wearable biosensors for healthcare monitoring. *Nat. Biotechnol.* **2019**, *37*, 389–406. [CrossRef]
59. Khan, Y.; Ostfeld, A.E.; Lochner, C.M.; Pierre, A.; Arias, A.C. Monitoring of vital signs with flexible and wearable medical devices. *Adv. Mater.* **2016**, *28*, 4373–4395. [CrossRef]
60. Patel, S.; Park, H.; Bonato, P.; Chan, L.; Rodgers, M. A review of wearable sensors and systems with application in rehabilitation. *J. Neuroeng. Rehabil.* **2012**, *9*, 1–17. [CrossRef]
61. Bodewein, L.; Schmiedchen, K.; Dechent, D.; Stunder, D.; Graefrath, D.; Winter, L.; Kraus, T.; Driessen, S. Systematic review on the biological effects of electric, magnetic and electromagnetic fields in the intermediate frequency range (300 Hz to 1 MHz). *Environ. Res.* **2019**, *171*, 247–259. [CrossRef] [PubMed]
62. Hariri, H.; Bernard, Y.; Razek, A. A traveling wave piezoelectric beam robot. *Smart Mater. Struct.* **2014**, *23*, 025013. [CrossRef]
63. Lemaire, E.; Moser, R.; Borsa, C.J.; Shea, H.; Briand, D. Green paper-based piezoelectric material for sensors and actuators. *Procedia Eng.* **2015**, *120*, 360–363. [CrossRef]
64. Hariri, H.; Bernard, Y.; Razek, A. Dual piezoelectric beam robot: The effect of piezoelectric patches positions. *J. Intell. Mater. Syst. Struct.* **2015**, *26*, 2577–2590. [CrossRef]
65. Khan, A.; Abas, Z.; Kim, H.S.; Kim, J. Recent progress on cellulose-based electro-active paper, its hybrid nanocomposites and applications. *Sensors* **2016**, *16*, 1172. [CrossRef]
66. Dagdeviren, C.; Joe, P.; Tuzman, O.L.; Park, K.I.; Lee, K.J.; Shi, Y.; Huang, Y.; Rogers, J.A. Recent progress in flexible and stretchable piezoelectric devices for mechanical energy harvesting sensing and actuation. *Extrem. Mech. Lett.* **2016**, *9*, 269–281. [CrossRef]
67. Stapleton, A.; Noor, M.R.; Sweeney, J.; Casey, V.; Kholkin, A.L.; Silien, C.; Gandhi, A.A.; Soulimane, T.; Tofail, S.A.M. The direct piezoelectric effect in the globular protein lysozyme. *Appl. Phys. Lett.* **2017**, *111*, 142902. [CrossRef]
68. Su, Q.; Quan, Q.; Deng, J.; Yu, H. A quadruped micro-robot based on piezoelectric driving. *Sensors* **2018**, *18*, 810. [CrossRef]
69. Pennes, H.H. Analysis of tissue and arterial blood temperatures in the resting human forearm. *J. Appl. Physiol* **1998**, *85*, 5–34. [CrossRef]
70. Sekkak, A.; Pichon, L.; Razek, A. 3-D FEM magneto-thermal analysis in microwave ovens. *IEEE Trans. Magn.* **1994**, *30*, 3347–3350. [CrossRef]
71. Clemens, M.; Gjonaj, E.; Pinder, P.; Weiland, T. Numerical simulation of coupled transient thermal and electromagnetic fields with the finite integration method. *IEEE Trans. Magn.* **2000**, *36*, 1448–1452. [CrossRef]
72. Harris, L.R.; Zhadobov, M.; Chahat, N.; Sauleau, R. Electromagnetic Dosimetry for Adult and Child Models within a Car: Multi-Exposure Scenarios. *Int. J. Microw. Wirel. Technol.* **2011**, *3*, 707–715. [CrossRef]
73. Gjonaj, E.; Bartsch, M.; Clemens, M.; Schupp, S.; Weiland, T. High-Resolution Human Anatomy Models for Advanced Electromagnetic Field Computations. *IEEE Trans. Magn.* **2002**, *38*, 357–360. [CrossRef]
74. Barchanski, A.; Steiner, T.; De Gersem, H.; Clemens, M.; Weiland, T. Local Grid Refinement for low-Frequency Current Computations in 3-D Human Anatomy Models. *IEEE Trans. Magn.* **2006**, *42*, 1371–1374. [CrossRef]
75. Hasgall, P.; Neufeld, E.; Gosselin, M.C.; Kingenböck, A.; Kuster, N. IT'IS Database for Thermal and Electromagnetic Parameters of Biological Tissues. 2012. Available online: https://bit.ly/30KwoL9 (accessed on 16 June 2022).
76. Gabriel, C.; Gabriel, S.; Corthout, E. The Dielectric Properties of Biological Tissues: II. Measurements in the Frequency Range 10 Hz to 20 GHz. *Phys. Med. Biol.* **1996**, *41*, 2251–2269. [CrossRef] [PubMed]
77. Bottauscio, O.; Roccato, P.E.; Zucca, M. Modeling the Dynamic Behavior of Magnetostrictive Actuators. *IEEE Trans. Magn.* **2010**, *46*, 3022–3028. [CrossRef]
78. Ouchetto, O.; Zouhdi, S.; Bossavit, A.; Griso, G.; Miara, B.; Razek, A. Homogenization of structured electromagnetic materials 689 and metamaterials. *J. Mater. Processing Technol.* **2007**, *181*, 225–229. [CrossRef]
79. Padilha, J.B.; Kuo-Peng, P.; Sadowski, N.; Batistela, N.J. Vector Hysteresis Model Associated to FEM in a Hysteresis Motor Modeling. *IEEE Trans. Magn.* **2017**, *53*, 1–4. [CrossRef]
80. Ren, Z.; Razek, A. New technique for solving three-dimensional multiply connected eddy-current problems. *IEE Proc. A Phys. Sci. Meas. Instr.* **1990**, *137*, 135–140. [CrossRef]
81. Sun, X.; Cheng, M.; Zhu, S.; Zhang, J. Coupled Electromagnetic-Thermal-Mechanical Analysis for Accurate Prediction of Du-695 al-Mechanical-Port Machine Performance. *IEEE Trans. Ind. Appl.* **2012**, *48*, 2240–2248. [CrossRef]
82. Ren, Z.; Razek, A. Boundary edge elements and spanning tree technique in three-dimensional electromagnetic field computation. *Int. J. Numer. Methods Eng.* **1993**, *36*, 2877–2893. [CrossRef]
83. Jiao, D.; Jin, J.-M. An effective algorithm for implementing perfectly matched layers in time-domain finite-element simulation of open-region EM problems. *IEEE Trans. Antennas Propag.* **2002**, *50*, 1615–1623. [CrossRef]
84. Carpes, W.P.; Pichon, L.; Razek, A. A 3D finite element method for the modelling of bounded and unbounded electromagnetic problems in the time domain. *Int. J. Numer. Model. Electron. Netw. Devices Fields* **2000**, *13*, 527–540. [CrossRef]

85. Sun, Q.; Zhang, R.; Zhan, Q.; Liu, Q.H. 3-D Implicit–Explicit Hybrid Finite Difference/Spectral Element/Finite Element Time Domain Method without a Buffer Zone. *IEEE Trans. Antennas Propag.* **2019**, *67*, 5469–5476. [CrossRef]
86. Chen, C.H.; Huang, C.Y.; Huang, Y.C. Improving the electromagnetic compatibility of electronic products by using response surface methodology and artificial neural network. *Microelectron. Int.* **2022**, *39*, 1–13. [CrossRef]
87. Yang, Y.; Zeng, S.; Li, X.; Hu, Z.; Zheng, J. Ultrahigh and Tunable Electromagnetic Interference Shielding Performance of PVDF Composite Induced by Nano-Micro Cellular Structure. *Polymers* **2022**, *14*, 234. [CrossRef]
88. Wang, G.; Wang, L.; Mark, L.H.; Shaayegan, V.; Wang, G.; Li, H.; Zhao, G.; Park, C.B. Ultralow-Threshold and Lightweight Biodegradable Porous PLA/MWCNT with Segregated Conductive Networks for High-Performance Thermal Insulation and Electromagnetic Interference Shielding Applications. *ACS Appl. Mater. Interfaces* **2018**, *10*, 1195–1203. [CrossRef]
89. Yao, B.; Hong, W.; Chen, T.; Han, Z.; Xu, X.; Hu, R.; Hao, J.; Li, C.; Li, H.; Perini, S.E.; et al. Highly Stretchable Polymer Composite with Strain-Enhanced Electromagnetic Interference Shielding Effectiveness. *Adv. Mater.* **2020**, *32*, e1907499. [CrossRef]
90. Yun, T.; Kim, H.; Iqbal, A.; Cho, Y.S.; Lee, G.S.; Kim, M.; Kim, S.J.; Kim, D.; Gogotsi, Y.; Kim, S.O.; et al. Electromagnetic Shielding of Monolayer MXene Assemblies. *Adv. Mater.* **2020**, *32*, e1906769. [CrossRef]
91. Song, W.-L.; Cao, M.-S.; Lu, M.-M.; Bi, S.; Wang, C.-Y.; Liu, J.; Yuan, J.; Fan, L.-Z. Flexible graphene/polymer composite films in sandwich structures for effective electromagnetic interference shielding. *Carbon* **2014**, *66*, 67–76. [CrossRef]
92. Song, W.-L.; Guan, X.-T.; Fan, L.-Z.; Cao, W.-Q.; Wang, C.-Y.; Cao, M.-S. Tuning three-dimensional textures with graphene aerogels for ultra-light flexible graphene/texture composites of effective electromagnetic shielding. *Carbon* **2015**, *93*, 151–160. [CrossRef]
93. Tan, Y.-J.; Li, J.; Gao, Y.; Li, J.; Guo, S.; Wang, M. A facile approach to fabricating silver-coated cotton fiber non-woven fabrics for ultrahigh electromagnetic interference shielding. *Appl. Surf. Sci.* **2018**, *458*, 236–244. [CrossRef]
94. Zhou, Q.; Yin, X.; Ye, F.; Mo, R.; Tang, Z.; Fan, X.; Cheng, L.; Zhang, L. Optically transparent and flexible broadband microwave metamaterial absorber with sandwich structure. *J. Appl. Phys. A* **2019**, *125*, 131. [CrossRef]
95. Han, M.; Yin, X.; Hantanasirisakul, K.; Li, X.; Iqbal, A.; Hatter, C.B.; Anasori, B.; Koo, C.M.; Torita, T.; Soda, Y. Anisotropic MXene aerogels with a mechanically tunable ratio of electromagnetic wave reflection to absorption. *Adv. Opt. Mater.* **2019**, *7*, 1900267. [CrossRef]
96. Cheng, J.; Li, C.; Xiong, Y.; Zhang, H.; Raza, H.; Ullah, S.; Wu, J.; Zheng, G.; Cao, Q.; Zhang, D. Recent Advances in Design Strategies and Multifunctionality of Flexible Electromagnetic Interference Shielding Materials. *Nano-Micro Lett.* **2022**, *14*, 80. [CrossRef]
97. Mohammad, M.; Wodajo, E.T.; Choi, S.; Elbuluk, M.E. Modeling and Design of Passive Shield to Limit EMF Emission and to Minimize Shield Loss in Unipolar Wireless Charging System for EV. *IEEE Trans. Power Electron.* **2019**, *34*, 12235–12245. [CrossRef]
98. Luo, Z.; Pathmanathan, M.; Han, W.; Nie, S.; Lehn, P.W. Analysis and design for constant current/constant voltage multi-coil wireless power transfer system with high EMF reduction. *IET Power Electron.* **2022**. [CrossRef]
99. Nie, S.; Pathmanathan, M.; Yakop, N.; Luo, Z.; Lehn, P.W. Field orientation basedthree-coil decoupled wireless transmitter for electricvehicle charging with large lateral receiver misalignment tolerance. *IET Power Electron.* **2021**, *14*, 946–957. [CrossRef]
100. Belyaev, I.; Dean, A.; Eger, H.; Hubmann, G.; Jandrisovits, R.; Kern, M.; Kundi, M.; Moshammer, H.; Lercher, P.; Müller, K.; et al. EUROPAEM EMF Guideline 2016 for the prevention, diagnosis and treatment of EMF-related health problems and illnesses. *Rev. Environ. Health* **2016**, *31*, 363–397. [CrossRef]
101. Feychting, M.; Ahlbom, A.; Kheifets, L. EMF AND HEALTH. *Annu. Rev. Public Health* **2005**, *26*, 165–189. [CrossRef]
102. Huang, P.C.; Cheng, M.T.; Guo, H.R. Representative survey on idiopathic environmental intolerance attributed to electromagnetic fields in Taiwan and comparison with the international literature. *Environ. Health* **2018**, *17*, 5. [CrossRef] [PubMed]
103. Point, S. Advocacy for A Cognitive Approach to Electrohypersensitivity Syndrome. *Skept. Inq.* **2020**, *44*, 47–50.
104. Baliatsas, C.; Van Kamp, I.; Lebret, E.; Rubin, G.J. Idiopathic environmental intolerance attributed to electromagnetic fields (IEI-EMF): A systematic review of identifying criteria. *BMC Public Health* **2012**, *12*, 643. [CrossRef] [PubMed]
105. Rubin, G.J.; Nieto-Hernandez, R.; Wessely, S. Idiopathic environmental intolerance attributed to electromagnetic fields (formerly 'electromagnetic hypersensitivity'): An updated systematic review of provocation studies. *Bio Electromagn.* **2010**, *31*, 1–11. [CrossRef]
106. Huang, P.-C.; Chiang, J.-C.; Cheng, Y.-Y.; Cheng, T.-J.; Huang, C.-Y.; Chuang, Y.-T.; Hsu, T.; Guo, H.-R. Physiological changes and symptoms associated with short-term exposure to electromagnetic fields: A randomized crossover provocation study. *Environ. Health* **2022**, *21*, 31. [CrossRef]
107. Genuis, S.J.; Lipp, C.T. Electromagnetic hypersensitivity: Fact or fiction? *Sci. Total Environ.* **2012**, *414*, 103–112. [CrossRef]